Tien et al., http://www.jcb.org/cgi/content/full/jcb.200910142/DC1

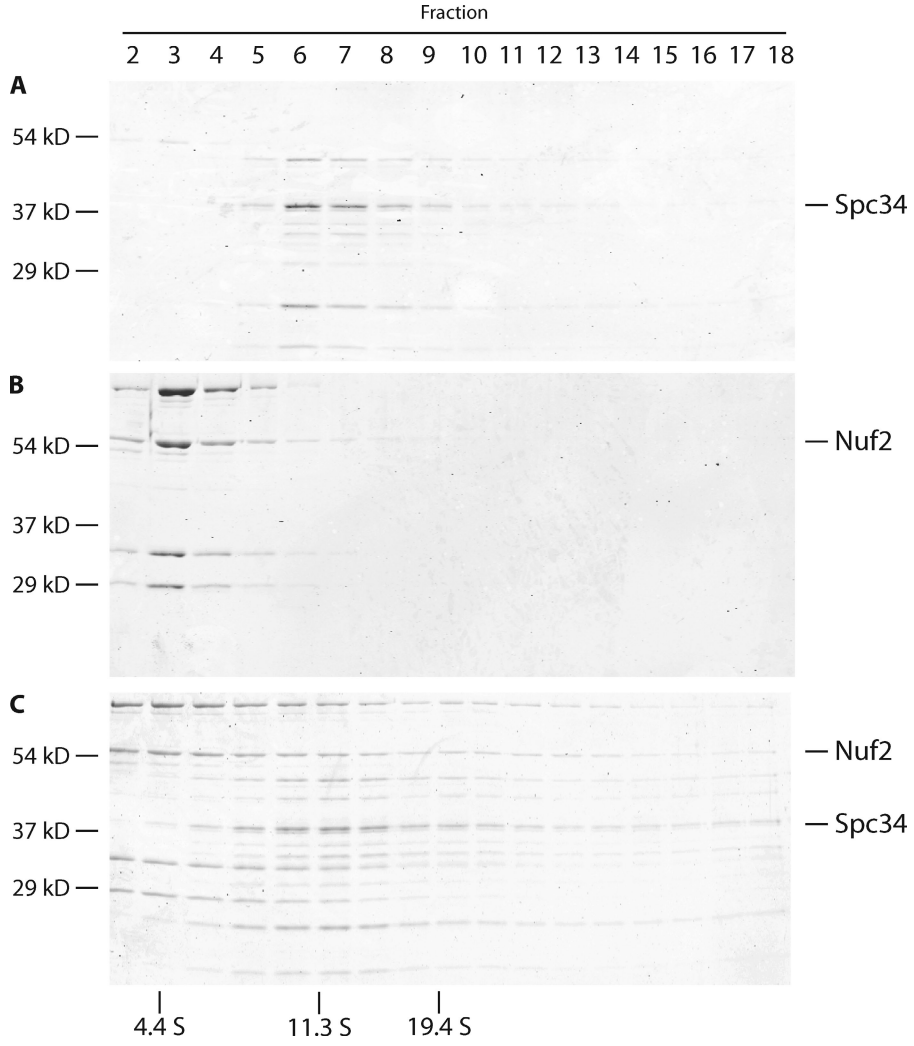

Figure S1. **Ndc80 and Dam1 complexes interact weakly free in solution.** The interaction between Ndc80 and Dam1 complexes free in solution was assayed by velocity sedimentation. 240 µl samples were layered onto 4.75 ml linear sucrose gradients (8–32%). Gradients were centrifuged at 189,000 *g* at 4°C for 6 h, and 265 µl fractions were collected. Fraction 1 is the top of the gradient. BSA (4.4S), catalase (11.3S), and thyroglobulin (19.4S) were used as standards. When assayed alone and together, Ndc80 complex and Dam1 complex had a sedimentation coefficient of 4.4S and 11.3S, respectively. Based on a Stokes radius of 9.9 nm, as determined by gel filtration, the molecular mass of the Dam1 complex was calculated to be ~470 kD (Siegel and Monty, 1966). Therefore, at the concentration in this assay, the 204-kD Dam1 complex exists primarily as a dimer free in solution. The positions of the Dam1 complex component Spc34 and the Ndc80 complex component Nuf2 are indicated on the right. (A–C) 2 µM Dam1 complex (A), 1 µM Ndc80 complex (B), and 2 µM Dam1 complex and 1 µM Ndc80 complex in combination (C) are shown.

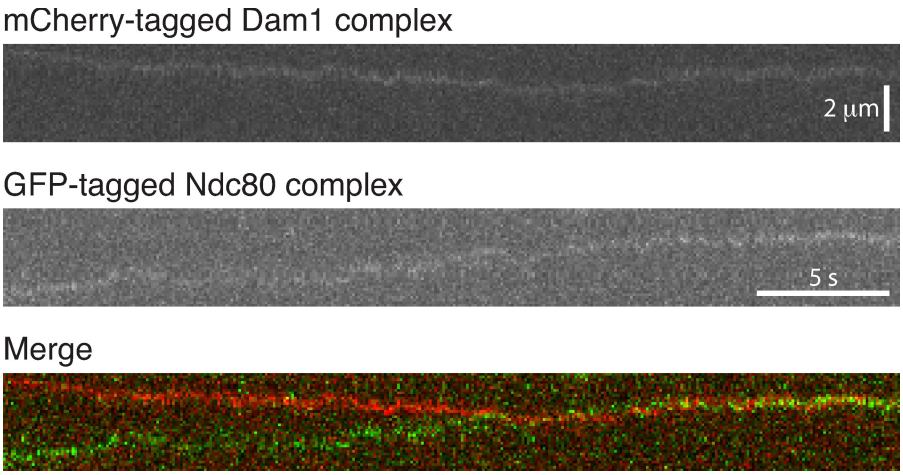

Figure S2. **The Ndc80 and Dam1 complexes interact on microtubules.** Representative kymograph showing the diffusion of 10 pM GFP-tagged Ndc80 complex and 2 pM mCherry-tagged Dam1 complex on microtubules. Both complexes are diffusive alone but appear to diffuse more slowly when they interact on microtubules.

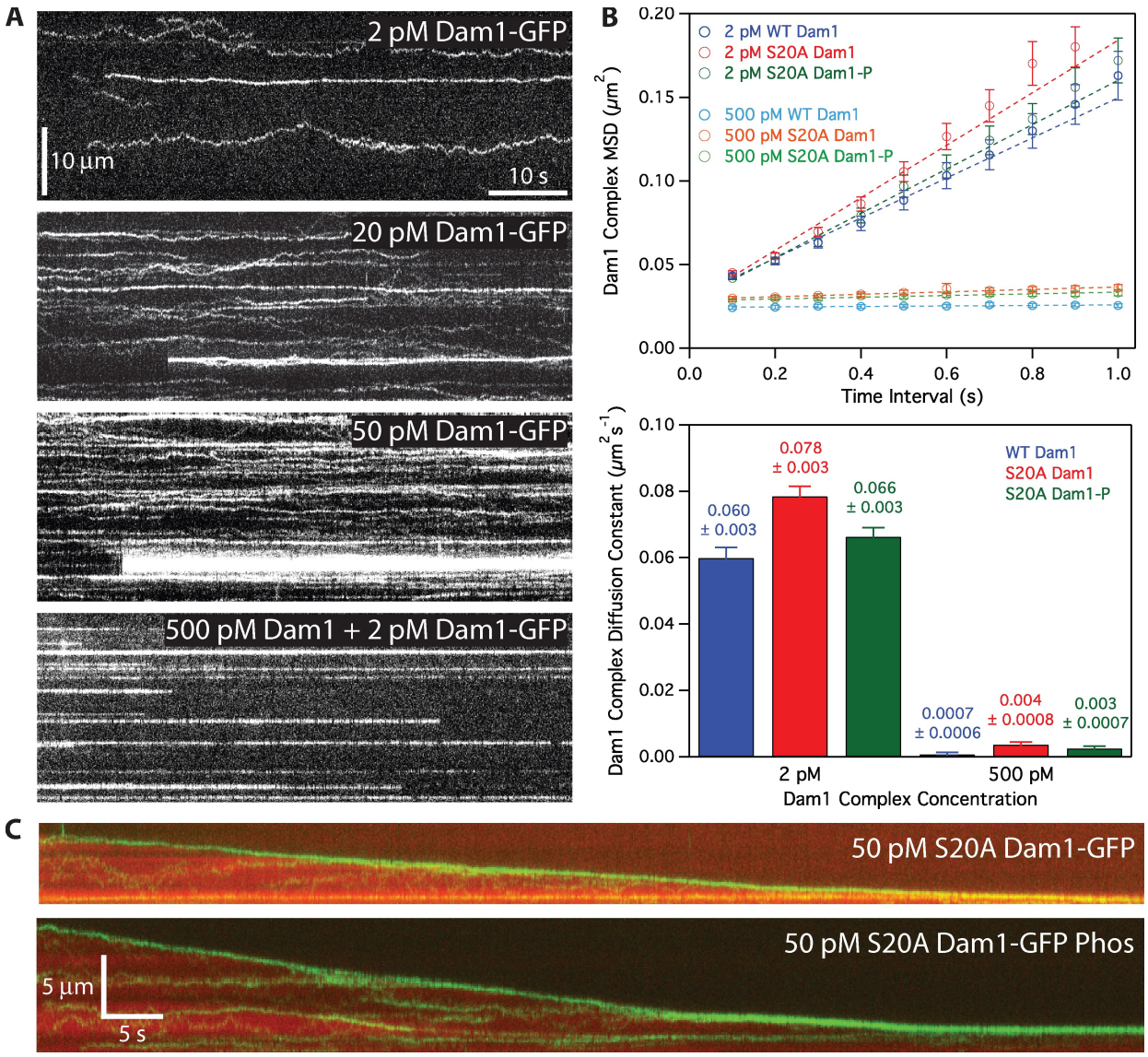

Figure S3. **The Dam1 complex oligomerizes on microtubules and tracks with disassembling tips.** (A) Representative kymographs showing changes in Dam1 complex behavior as it oligomerizes on microtubules. At 2 pM GFP-tagged Dam1 complex, single monomers were discernable. At 20 and 50 pM, slowly diffusing oligomers were seen as lines. At 500 pM Dam1 complex, the behaviors of individual oligomers were traced by visualizing a small proportion of labeled complex. Concentrations are of free complexes in solution. (B) Oligomerization of Dam1 complex slows its diffusion on taxol-stabilized microtubules, and oligomerization of S20A Dam1 complex is not abolished by Ipl1 phosphorylation. (top) Mean-squared displacement (MSD) is plotted against time for 2 pM wild-type (WT) Dam1 complex (blue markers; n = 188), 2 pM S20A Dam1 complex (red markers; n = 327), 2 pM Ipl1-phosphorylated S20A Dam1 complex (green markers; n = 346), 500 pM wild-type Dam1 complex (light blue markers; n = 129), 500 pM S20A Dam1 complex (orange markers; n = 188), and 500 pM Ipl1-phosphorylated S20A Dam1 complex (light green markers; n = 231). At 500 pM Dam1 complex, the behaviors of individual oligomers were traced by visualizing a small proportion of labeled complex. Markers are mean values ± SEM. Dotted lines show the weighted linear fits used to determine diffusion constants, D. (bottom) Diffusion constants derived from mean-squared displacement versus time plots are summarized as a bar graph. Wild-type Dam1 complex (blue bars), S20A Dam1 complex (red bars), and Ipl1-phosphorylated S20A Dam1 complex (green bars) are shown. Error bars indicate SEM. (C) Representative two-color kymographs demonstrating the tip-tracking ability of Ipl1-phosphorylated S20A Dam1 complex. Movement of 50 pM GFP-tagged unphosphorylated and phosphorylated S20A Dam1 complex (green) is shown on disassembling microtubules (red).

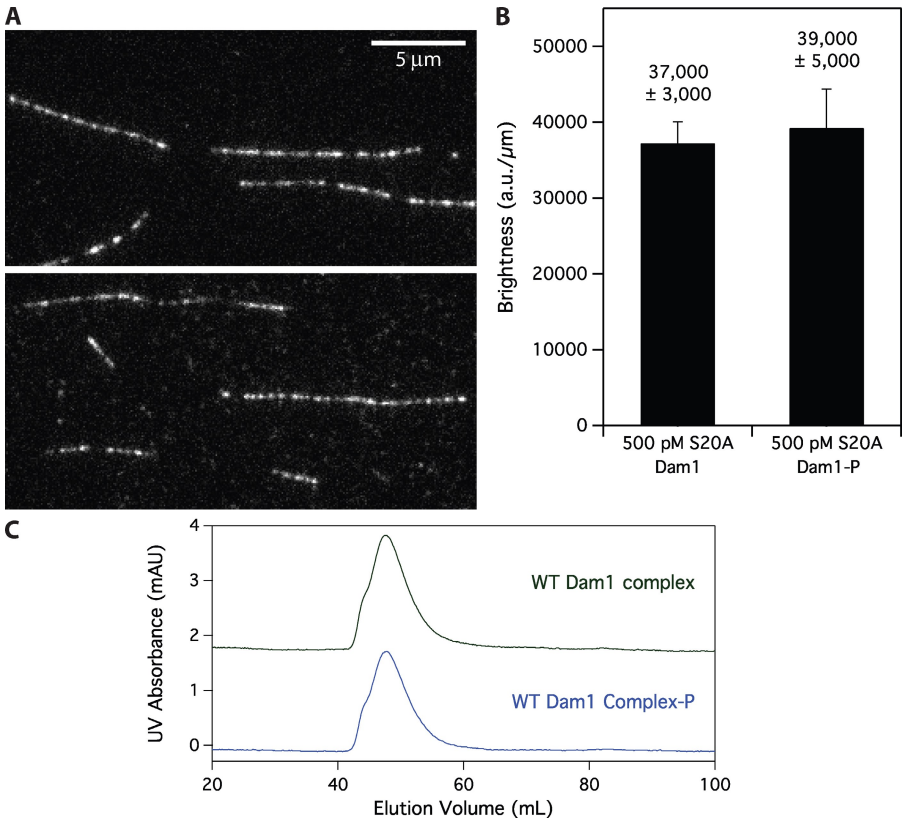

Figure S4. **Phosphorylation does not affect microtubule binding of S20A Dam1 complex and does not cause disassembly of wild-type Dam1 complex.** (A) Representative images of mCherry-tagged S20A Dam1 complex on microtubules. (top) 500 pM S20A Dam1 complex. (bottom) 500 pM Ipl1-phosphorylated S20A Dam1 complex. (B) Image means of mCherry brightness per unit length microtubules for unphosphorylated (n = 6 images, representing 68 microtubules, totaling 790 µm) and phosphorylated (n = 7 images, representing 51 microtubules, totaling 754 µm) S20A Dam1 complex. Error bars indicate SEM. (C) Unphosphorylated and Ipl1-phosphorylated wild-type (WT) Dam1 complexes each migrate as a single peak during gel filtration and elute at a volume consistent with previously reported values (Gestaut et al., 2008). The elution profile for unphosphorylated Dam1 complex is offset vertically by 2 mAU.

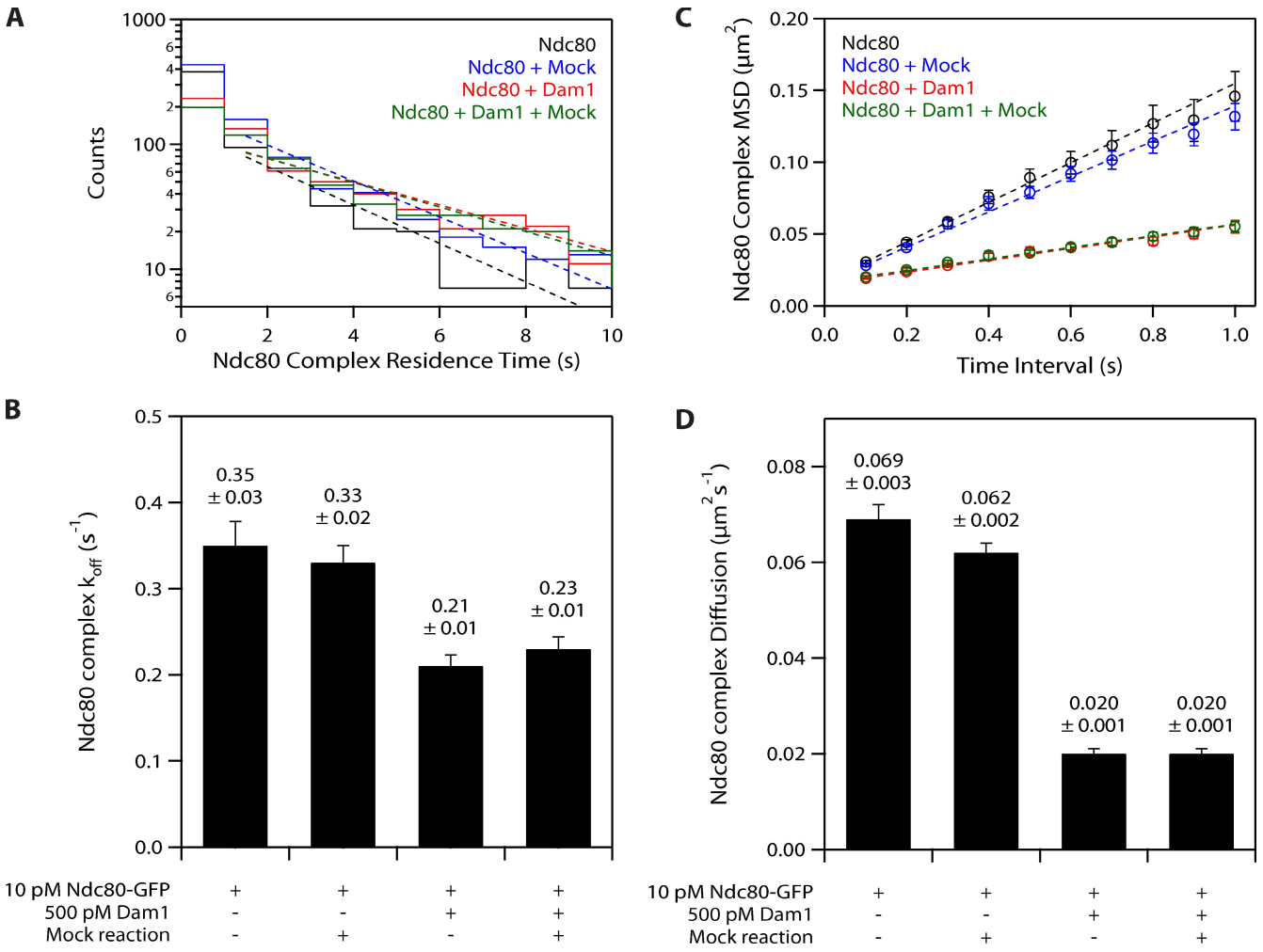

Figure S5. **Residual components of Ipl1 phosphorylation reactions have no effect on the behavior of the Ndc80 complex on microtubules.** Mock Ipl1 phosphorylation reactions were performed with BSA in place of Dam1 complex and added to TIRF assays at concentrations as in Fig. 6 (63 pM Ipl1, 63 pM Sli15, and 1.3 μM ATP). (A) Residence time distributions of 10 pM GFP-tagged Ndc80 complex on microtubules alone (black histogram; *n* = 692), with mock reaction (blue histogram; *n* = 869), 500 pM Dam1 complex (red histogram; *n* = 752), and 500 pM Dam1 complex and mock reaction (green histogram; *n* = 699). Dotted lines show the weighted exponential fits used to determine dissociation rate constants, k_{off}. (B) Dissociation rate constants derived from histograms are summarized as a bar graph. (C) Mean-squared displacement (MSD) is plotted against time for 10 pM GFP-tagged Ndc80 complex on microtubules alone (black markers; *n* = 472), with mock reaction (blue markers; *n* = 670), 500 pM Dam1 complex (red markers; *n* = 636), and 500 pM Dam1 complex and mock reaction (green markers; *n* = 586). Dotted lines show the weighted linear fits used to determine diffusion constants, D. (D) Diffusion rate constants derived from mean-squared displacement versus time plots are summarized as a bar graph. Error bars indicate SEM.

References

Gestaut, D.R., B. Graczyk, J. Cooper, P.O. Widlund, A. Zelter, L. Wordeman, C.L. Asbury, and T.N. Davis. 2008. Phosphoregulation and depolymerization-driven movement of the Dam1 complex do not require ring formation. *Nat. Cell Biol.* 10:407–414. doi:10.1038/ncb1702

Siegel, L.M., and K.J. Monty. 1966. Determination of molecular weights and frictional ratios of proteins in impure systems by use of gel filtration and density gradient centrifugation. Application to crude preparations of sulfite and hydroxylamine reductases. *Biochim. Biophys. Acta.* 112:346–362. doi:10.1016/0926-6585(66)90333-5